Survival window for atomic tunneling ionization with elliptically polarized laser fields

Kai-yun Huang,[1,3] Qin-zhi Xia,[1] and Li-Bin Fu[1,2,*]

[1]*National Laboratory of Science and Technology on Computational Physics, Institute of Applied Physics and Computational Mathematics, Beijing 100088, China*

[2]*HEDPS, Center for Applied Physics and Technology, Peking University, Beijing 100084, China*

[3]*Graduate School, China Academy of Engineering Physics, Beijing 100088, China*

(Received 21 December 2012; published 20 March 2013)

We find a fraction of atoms remain unionized after the laser pulse when the tunneled electrons are released in a certain window of initial field phase and transverse velocity. The survival window shifts with laser polarization ellipticity and its width varies with respect to laser intensity and atomic ionization potential. Neutral atom yield can be calculated by summing up tunneling probabilities in the window. Our theory can quantitatively reproduce the distribution of the survival yields vs laser ellipticity observed for helium in experiment. For other atom species with smaller ionization potential such as magnesium, our theory predicts a wider distribution than the strong-field approximation model while closer to the three-dimensional semiclassical electron ensemble simulations, indicating the important role of the Coulomb effects.

DOI: 10.1103/PhysRevA.87.033415 PACS number(s): 32.80.Rm, 42.50.Hz, 33.80.Rv

I. INTRODUCTION

Tunneling and recollision, the phenomena that the electron sets free from an atom or molecule by a strong field and then collides with the core driven by the oscillating field, are at the heart of strong-field physics [1]. Tunnel ionization occurs when the optical frequency of the field is low enough that the electron has time to tunnel through the suppressed Coulomb potential. Recollision plays an important role in enhancing above threshold ionization (ATI) signal [2], high-order harmonic generation (HHG) [3,4], as well as nonsequential double-ionization (NSDI) process [5,6]. Recently, it has been shown that the tunneled electron can be left in high-lying Rydberg state at the end of the laser pulse [7–14], leading to many neutral atoms or highly excited singly charged ions surviving the strong field. The experiments found that the signal of neutral atoms is sensitive to the polarization of laser field. For the helium (He) [7], the experimental results show that the fraction of Rydberg state drastically decreases for small deviation from linear polarization and becomes zero for high ellipticity. Semiclassical simulations are in good agreement with the experimental results and indicate that the recollision is essential for the creation of the Rydberg atoms.

The yields of neutral atoms and creating Rydberg atoms in laser field are of great importance in both fundamental and applied physics, such as acceleration of neutral atoms or molecules [14,15], controlled collision [16–19], atomic nanofabrication [20,21], and atom optics [22]. It is no doubt that Coulomb force dominates the evolution of the electron which tunneled without ionization. However, how the Coulomb effect takes the role in the neutral atoms survival phenomenon is still unresolved [23].

In this paper, we investigate neutral atoms survival rate for elliptical laser fields based on a semiclassical quasistatic model and focus on the Coulomb effect. Our simulations reproduced the experimental observations for He quantitatively. We found a fraction of atoms remain unionized after the laser pulse when the tunneled electrons are released in a certain window of initial field phase and transverse velocity. We name this window as the survival window. The boundary of the survival window can be obtained under strong-field approximation (SFA) with Coulomb correction. The yields rate of neutral excited atoms will then be evaluated by summing up the probabilities within the survival window. The theoretical results quantitatively reproduce the distribution of helium. For atom species with smaller ionization potential, our theory predicts a wider distribution than the SFA model while closer to the three-dimensional (3D) semiclassical electron ensemble simulations, indicating the important role of the Coulomb effects. The deviations between theoretical results and numerical simulations are due to the multiple scattering orbits of some electrons which cannot be approximated by SFA.

Our paper is organized as follows. In Sec. II, we present our model. Section III is our main results. Finally, we draw a conclusion in Sec. IV.

II. MODEL CALCULATION

In order to achieve deep insight into recollision dynamics behind the neutral atoms survival, we perform 3D semiclassical electron ensemble simulations including tunneling effect and all the correlations (for the details see, e.g., Refs. [24,25]). Briefly, in the model, the electric field rotates clockwise or counterclockwise as it propagates along the z axis. The tip of the electric-field vector describes an ellipse in the x-y plane. At time t_0, electron tunnels out from the nucleus parallel to the instantaneous electric-field direction with zero initial parallel velocity. The initial tunneling position along the laser polarization direction can be derived from the Landau's effective potential theory [26]. Besides, the electron also has an initial transverse velocity $v_\perp$ perpendicular to the instantaneous electric field, and $v_\perp$ satisfies Gussian-like distribution. Each electron trajectory is weighted by the ADK ionization rate $w(\chi,t_0,v_\perp) = w(0)w(v_\perp)$ [27]. $w(v_\perp) = \frac{2\sqrt{2I_p}v_\perp}{\varepsilon_{t_0}} \exp(-\frac{\sqrt{2I_p}v_\perp^2}{\varepsilon_{t_0}})$ is the distribution of initial transverse velocity $v_\perp$, and $w(0) = \varepsilon_{t_0}^{(1-2/\sqrt{2I_p})} \exp(-\frac{2(\sqrt{2I_p})^3}{3\varepsilon_{t_0}})$ depends

*lbfu@iapcm.ac.cn

on the instantaneous field strength ε_{t_0} at the time when the electron releases and the ionization potential I_p. The evolution of the tunneled electron is governed by Newton's equations of motion, $\frac{d^2\vec{r}}{dt^2} = -\frac{\vec{r}}{r^3} - \vec{\varepsilon}$.

In the simulation, the electric field of the laser is given by

$$\vec{\varepsilon}(t) = \frac{\varepsilon_0 f(t)}{\sqrt{1+\chi^2}}[\cos(\omega t)\vec{e}_x + \chi \sin(\omega t)\vec{e}_y], \qquad (1)$$

where ε_0 and ω are the amplitude and frequency of the laser field, respectively. χ is the laser ellipticity. The envelope function $f(t)$ is the slowlyvarying pulse envelope: $f(t) = 1$ for $t \leqslant 8T$, and adiabatically ramped off within three laser cycles, namely $f(t) = \cos^2\frac{(t-8T)\pi}{6T}$ for $8T < t \leqslant 11T$. Here, $T = 2\pi/\omega$ is the oscillating period of the laser field. In our calculation the wavelength is $\lambda = 800$ nm ($\omega = 0.056$) a.u.

From Landau's effective potential theory [26] and considering the instantaneous direction of field, the initial position can be given by $x_0 = -\frac{\eta_0}{2}\cos\theta, y_0 = -\frac{\eta_0}{2}\sin\theta, z_0 = 0$, θ is the angle between the direction of the electric field and x axis, in which $\eta_0 = \frac{I_p+\sqrt{I_p^2-2\varepsilon_{t_0}}}{\varepsilon_{t_0}}$, and $\varepsilon_{t_0} = \frac{\varepsilon_0}{\sqrt{1+\chi^2}}\sqrt{\cos^2(\omega t_0) + \chi^2\sin^2(\omega t_0)}$. The initial velocity is then $v_{x0} = -v_\perp \sin\beta \sin\theta, v_{y0} = v_\perp \sin\beta \cos\theta, v_{z0} = v_\perp \cos\beta$ with the distribution $w(v_\perp)$. The angle between the transverse velocity and the z axis is β.

With the model we calculate yields of neutral excited He* atoms and Mg* atoms for different ellipticities. The laser intensity for helium is chosen as $I = 1$ PW/cm^2 in order to compare with the experiment in Ref. [7], and for magnesium intensity is $I = 0.0116$ PW/cm^2. The yields of neutral atoms are normalized as following $w_{\text{atom}^*} = \frac{\sum_{E_f<0} w(\chi,t_0,V_\perp)}{\max\sum_{E_f<0} w(\chi,t_0,V_\perp)}$; E_f is the final energy of the tunneled electron.

The normalized yields of neutral excited He* atoms and Mg* atoms for different ellipticities are plotted in the upper panels (in Fig. 1): the left is for He* and the right is for Mg*, respectively. The results for helium obtained by our model are in good agreement with the experimental data, and consist with the prediction of the SFA model for which the neutral atom yield is a Gaussian distribution as a function of ellipticity χ with a standard deviation $\sigma_0 = \sqrt{\frac{3}{3+\gamma^2}}\frac{\omega}{\sqrt{2\varepsilon_0}(2I_p)^{1/4}}$, where γ is the Keldysh parameter $\gamma = \frac{\omega\sqrt{2I_p}}{\varepsilon_0}$ [23]. At $\chi = 0$, the yield of He* is maximum. Near $\chi = 0.3$, the yield of survival helium decreases to zero.

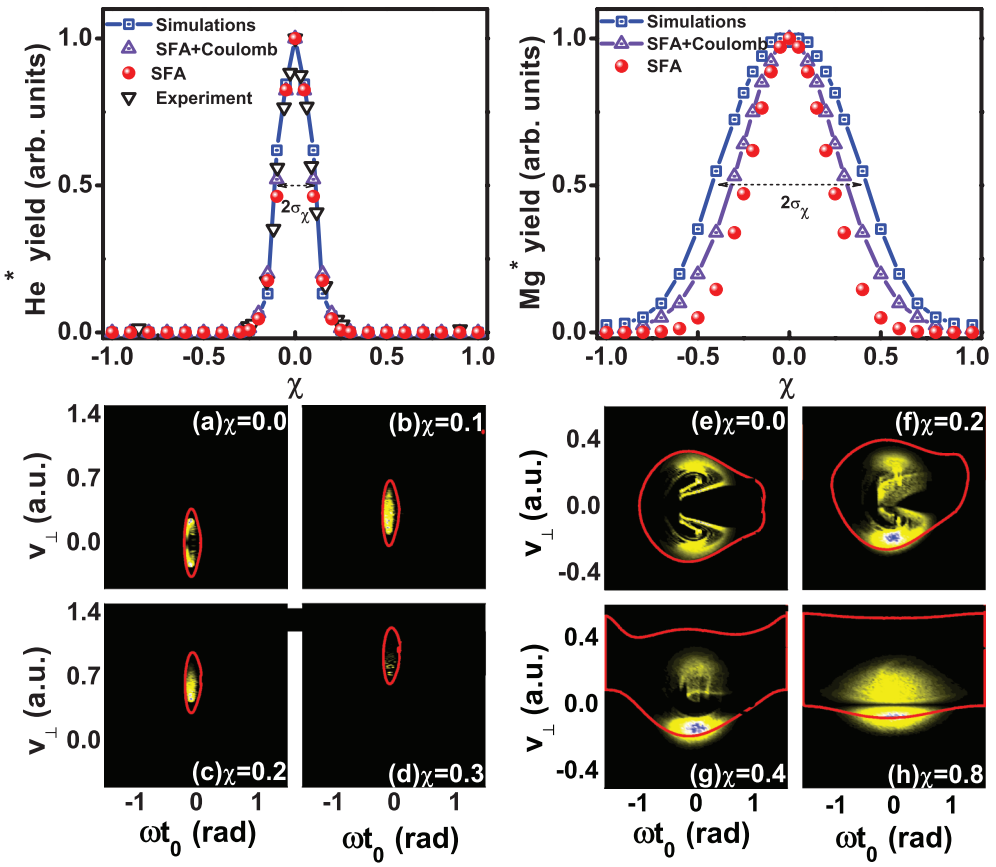

FIG. 1. (Color online) Upper panels: yield of survival He* atoms (left) and Mg* atoms (right) versus ellipticity. Black triangles are experimental data from Ref. [7], blue squares are numerical simulations, purple triangles are obtained by SFA with Coulomb correction, and the red balls are pure SFA results. The parameters used for He* atom are $I = 1$ PW/cm^2,$\omega = 0.056$ a.u. and for Mg* atom is $I = 0.0116$ PW/cm^2,$\omega = 0.056$ a.u. Lower panels: distribution of initial transverse velocity and tunneling phase for surviving He* atoms (left) and Mg* atoms (right) at different ellipticities. The bright regimes are numerical results and red curves indicate the boundary for unionized window predicted by our theoretical analysis (see text for details).

Different from helium, the yield of Mg* decreases slowly with increasing ellipticity. And even for circular polarization, the survival yield does not drop down to zero. Compared with the results from the SFA model, the distribution of neutral atom yield w_{Mg^*} is much wider. This fact implies the Coulomb effect may play an important role in the neutral atom surviving process for atoms with smaller ionization potential.

III. COULOMB EFFECTS AND SURVIVAL WINDOW

A. Survival window

The Coulomb effects are twofold: the Coulomb potential of the tunneled electron at birth time and the Coulomb scattering effect during the recollision process. Considering the Coulomb potential, the energy of tunneled electrons at the birth time can be expressed by $E_0 = \frac{1}{2}[\vec{v}_0 + \vec{A}(\omega t_0)]^2 - \frac{1}{r_0}$, where r_0 is the exit point from tunneling. Then, the tunneled electron will be accelerated in the consequent scattering processes mediated by the Coulomb and laser fields. The energy gain can be expressed by

$$\Delta E = -\int_{t_0}^{t_{\mathrm{final}}} \frac{xA_x + yA_y}{r^3} dt. \tag{2}$$

The electron orbit $\vec{r}(t) = (x(t), y(t), z(t))$ can be obtained under SFA by solving Newton equations $\frac{d^2\vec{r}}{dt^2} = -\vec{\varepsilon}$ with initial condition $\vec{r}_0 = (-\frac{\eta_0}{2}\cos\theta, -\frac{\eta_0}{2}\sin\theta, 0)$. Under this approximation, the final energy of the electron is $E_f = E_0 + \Delta E$. When the tunneled electrons are released in a certain window of initial field phase ωt_0 and transverse velocity $v_\perp$, the final energy $E_f < 0$. We call this window the survival window. The boundary lines $E_0 + \Delta E = 0$ of the survival window are plotted in Figs. 1(c) and 1(d) (labeled by red lines) for He and Mg, respectively.

We can see that almost all of the survival events come from the survival window confined by the boundary $E_0 + \Delta E = 0$. Hence one can estimate the yields rate of neutral excited atoms by summing up the probabilities within the survival window, i.e., the total yield of survival atoms can be approximately estimated by the following formula:

$$w'_{atom^*} = \oint_S w(\chi, t_0, v_\perp) dS, \tag{3}$$

where S is the area of the survival window.

It is interesting that the field phases ωt_0 for the survival window are changed slightly when ellipticity varies. But at the same time, the transverse velocities $v_\perp$ for the survival window change clearly with ellipticity varying. The field phases ωt_0 determine the tunneling probability $w(0)$, and for the same atom and laser intensity it does not change for a given phase ωt_0. Hence the $w(v_\perp)$ plays an important role on the survival rate.

In Fig. 2, we plot the distribution $w(v_\perp)$ and the survival windows (at $\omega t_0 = 0$) for different ellipticities for He* and Mg*, respectively. Obviously, the behaviors of the survival windows for He* and Mg* are quite different. This difference gives rise to different dependence of survival rates for He* and Mg* on polarization of laser fields.

The shadow areas in Fig. 2 correspond to the survival window. The maximum velocity $v_{\max}$ and the minimum velocity $v_{\min}$ of the window are represented by green circle and blue circle, respectively. The red circle labels the drift velocity $v_d = \frac{\chi\varepsilon_0}{\omega\sqrt{1+\chi^2}}$, which is in the middle of the window and moves with the window as ellipticity increases. We can see that the survival window drifts drastically to the large transverse velocity for He*, but for Mg* the drift of the survival window is not notable. At the same time, from Figs. 2(d)–2(f), one can see the pattern structure is complex for Mg*.

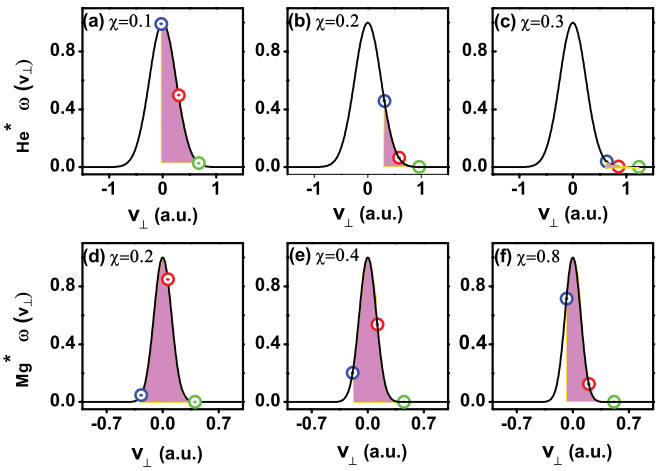

FIG. 2. (Color online) Distribution of initial transverse velocity for tunneling electron at different ellipticities. The first row is for He* and the second row is for Mg*. The shadow area is the velocity window for survival atoms. The maximum velocity and the minimum velocity of the window are represented by green circle and blue circle, respectively. The red circle is the drift velocity.

The difference between He* and Mg* can be illustrated by the width of the survival window which is denoted by $\Delta = v_{\max} - v_{\min}$. For He*, $\Delta_{H_e} \ll v_d^{\max}$ ($v_d^{\max} = \frac{\varepsilon_0}{\sqrt{2}\omega}$), but for Mg*, $\Delta_{M_g} \sim v_d^{\max}$. When the survival window is narrow, i.e., $\Delta \ll v_d^{\max}$, the probability $w(v_d)$ can serve as the mean of probabilities of survival events, so that Keller's formula obtained with SFA works well. But for broad survival window, i.e., $\Delta \sim v_d^{\max}$, we need to include the Coulumb effect to calculate the total yield of survival atoms.

Perhaps, for a narrow window case, the $w(v_d)$ can serve as the mean of probabilities of survival events, but for a broad window, the pattern structure within the window may play the role. As we mentioned before, the window width Δ is the distance between two peak points that correspond to initial phase $\omega t_0 = 0$ on boundary line $E_f = 0$. According to Ref. [28], the energy gain ΔE in combined laser and Coulomb field can be obtained by setting that the tunneled electron travels along a straight trajectory generated by the constant field ε_{t_0}. Then with the initial energy, we get the final energy E_f, which is a quadratic function of initial transverse velocity $v_\perp$. Let $\omega t_0 = 0$ and $E_f = 0$; we get $\Delta = 2\sqrt{\frac{2\varepsilon_0}{I_p} - \frac{\pi^2\varepsilon^2}{8I_p^3}}$. Due to $I_p \gg \varepsilon_0$, we omit the second term in the radical and get $\Delta/v_d^{\max} \propto \frac{\omega}{\sqrt{\varepsilon_0 I_p}}$. Hence we can vary the window by changing atom species.

It is convenient to employ the full width at half maximum (FWHM) denoted as σ_χ to describe the survival yield w_{atom} versus ellipticity. Using it we estimate the effect of an elliptically polarized field on different atoms. In Fig. 3 we

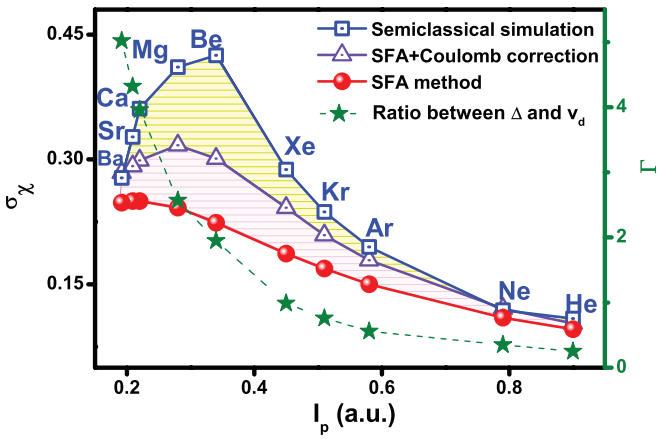

FIG. 3. (Color online) Full width at half maximum (FWHM) σ_χ for each atom at typical laser intensity. The red balls represent the result of formula $\sigma_\chi^{\rm SFA} = \sqrt{\frac{6\ln 2}{3+\gamma^2}}\frac{\omega}{\sqrt{2\varepsilon_0(2I_p)^{1/4}}}$ deduced from SFA model, the purple triangles represent the result of Eq. (3) obtained from SFA+Coulomb correction model, and the blue squares are our semiclassical simulation. Γ (denoted by green star) is the ratio between the width of phase window Δ and the drift velocity v_d for different atoms.

give the FWHM of many atoms. Each atom is calculated at corresponding typical field intensity I_T (see Table I), with which the total ADK ionization rate for the atom is equal to each other as the field is linearly polarized. The blue squares and purple triangles represent our numerical results and theoretical results of Eq. (3), respectively. The red balls are results of SFA obtained from Keller's formula [23]. Here, the ratios $\Gamma = \Delta/v_d^{\rm max}$ for different atoms are plotted with green stars.

From this figure, we find the theoretical results given by Eq. (3) are consistent with the numerical results for narrow window cases, but with the window width increasing the numerical results are higher than the theoretical ones. The deviation of theoretical results from numerical results implies that the recollision motions are more complex for broad survival window cases.

TABLE I. Corresponding typical laser intensity I_T for each atom.

Atom	He	Ne	Ar	Kr	Xe
I_T (PW/cm^2)	1.0	0.634	0.206	0.1268	0.0783
Atom	Be	Mg	Ca	Sr	Ba
I_T (PW/cm^2)	0.0257	0.0116	0.0042	0.0034	0.0024

B. Chaotic scattering for broad survival window

Indeed, some of electrons inside the window might experience multiple forward and backward scatterings. Their orbits are essentially chaotic [29,30] and cannot be described by SFA. In a linearly polarized laser field the classical electron energy has been calculated by averaging over the fast chaotic oscillation, and the probability of ionization from the ground state of the atom to a lower-lying state in the continuum has been acquired using the Landau-Dykhne approximation in Ref. [30]. Similarly, in the elliptically polarized laser fields, those electrons acquire additional energy during the chaotic scattering and finally get ionized. This fact makes the unionized area become irregular and form unionized islands in the window. In Figs. 1(a)–1(d) and 1(e)–1(h) (He and Mg, respectively), one can clearly see the islands structure obtained by 3D semiclassical model calculations.

For the atoms with broad survival windows, the survival rates depend on the survival islands within the survival window. The migrating of survival islands can be controlled through changing ellipticity; this can be seen from Figs. 4(b)–4(d). In Fig. 4(a) we plot dependence of Mg* yield on ellipticity for laser intensity 0.04 PW/cm^2. We see that the dependence

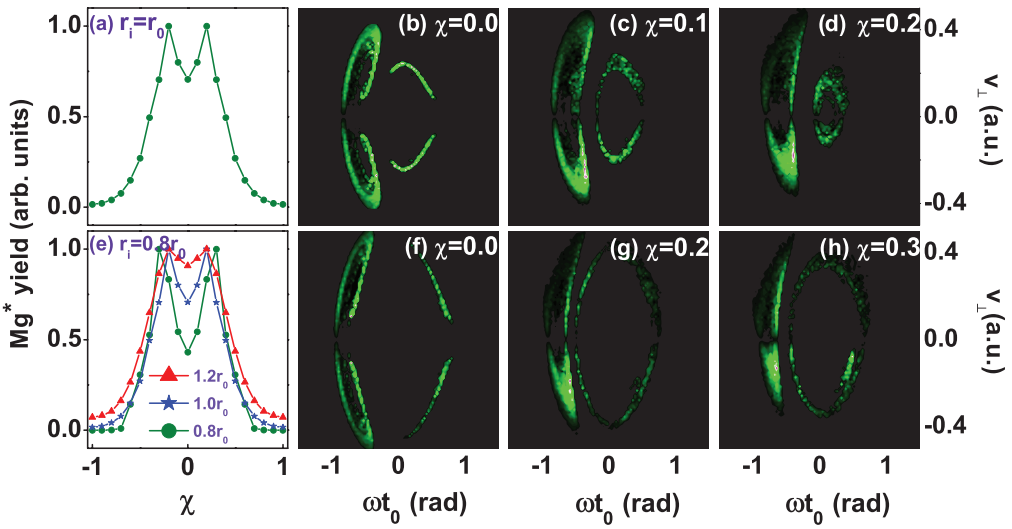

FIG. 4. (Color online) Behavior shown by magnesium subject to elliptically polarized field. The laser intensity is $I = 0.04$ PW/cm^2. In the first row, (a) is the dependence of Mg* yield on ellipticity. Images (b)–(d) are the migrating of survival islands with ellipticity when the tunneling position is $r_i = r_0$. In the second row, (e) is the dependence of Mg* yield on ellipticity as the tunneling position is $r_i = 1.2r_0$ (red triangle line), $r_i = 1.0r_0$ (blue star line), and $r_i = 0.8r_0$ (green dot line), respectively. Panels (f)–(h) are obtained when the tunneling position is $r_i = 0.8r_0$.

of Mg^* yield on ellipticity deviates from Gaussian-like and becomes more complex. The yield of Mg^* atom at ellipticity $\chi = 0$ drops down seriously and two peaks appear at $\chi = \pm 0.2$.

The chaotic orbits of a nonlinear system are always sensitive to its initial conditions and system parameters. The sensitive behaviors of migrating of survival islands to the ellipticity show typical nonlinear behaviors. Of course, the survival islands migrating will be sensitive to the initial conditions, which should be used to calibrate the tunnel exit position. To study the sensitivity of survival islands on initial condition, we artificially change the tunnel position r_0 to a different value r_i. In the simulated test, we set $r_i = 0.8r_0$ and $r_i = 1.2r_0$, respectively. The dependence of Mg^* yield on ellipticity and survival windows with the above three different initial positions are plotted in Fig. 4(e). One can find the yield of Mg^* atom at ellipticity $\chi = 0$ is sensitive to the initial position. In Figs. 4(f)–4(h), we illustrate survival islands for $r_i = 0.8r_0$ and their migrating with ellipticity changing. Comparing with cases of $r_i = r_0$ [in Figs. 4(b)–4(d)], one can find that the migrating behaviors of survival islands are also sensitive to the initial condition.

IV. SUMMARY

We found there is a survival window of initial field phase and transverse velocity, in which a fraction of tunneled electrons can survive after the laser pulse. The survival window shifts with polarization ellipticity of laser field and its width varies with respect to laser intensity and atomic species. The width of the survival window determines the dependence of neutral atoms survival rate on ellipticity. For narrow window cases, the dependence of neutral atoms survival rate on ellipticity is dominated by the drifting of the survival window, and Coulomb effect will not be apparent (e.g., for helium experiment). But for broad window cases, the survival rate of neutral atoms depends on migrating of survival islands within the survival window. For these cases, the neutral atom yield as a function of ellipticity will deviate from Gaussian distribution. The migrating of survival islands indicates the recollision orbits are sensitive to the initial conditions, which is a typical chaotic behavior induced by the nonlinearity of Coulomb potential. This feature can be used for calibration of the tunneling geometry.

ACKNOWLEDGMENTS

We are grateful to Jie Liu for numerous discussions. This work is supported by the National Fundamental Research Program of China (Contracts No. 2007CB814800 and No. 2011CB921503), the National Natural Science Foundation of China (Contracts No. 10725521, No. 91021021, No. 11075020, and No. 11078001).

[1] P. B. Corkum, Phys. Today **64**, 36 (2011).
[2] J. Wassaf, V. Véniard, R. Taïeb, and A. Maquet, Phys. Rev. A **67**, 053405 (2003).
[3] A. Scrinzi, M. Y. Ivanov, R. Kienberger, and D. M. Villeneuve, J. Phys. B **39**, R1 (2006).
[4] T. Brabec, *Strong Field Laser Physics* (Springer, New York, 2008).
[5] W. Becker, Rev. Mod. Phys. **84**, 1011 (2012).
[6] B. Feuerstein *et al.*, Phys. Rev. Lett. **87**, 043003 (2001).
[7] T. Nubbemeyer, K. Gorling, A. Saenz, U. Eichmann, and W. Sandner, Phys. Rev. Lett. **101**, 233001 (2008).
[8] T. Nubbemeyer, U. Eichmann, and Sandner, J. Phys. B **42**, 134010 (2009).
[9] B. Manschwetus, T. Nubbemeyer, K. Gorling, G. Steinmeyer, U. Eichmann, H. Rottke, and W. Sandner, Phys. Rev. Lett. **102**, 113002 (2009).
[10] K. N. Shomsky, Z. S. Smith, and S. L. Haan, Phys. Rev. A **79**, 061402(R) (2009).
[11] B. Ulrich, A. Vredenborg, A. Malakzadeh, M. Meckel, K. Cole, M. Smolarski, Z. Chang, T. Jahnke, and R. Dörner, Phys. Rev. A **82**, 013412 (2010).
[12] J. McKenna, S. Zeng, J. J. Hua, A. M. Sayler, M. Zohrabi, N. G. Johnson, B. Gaire, K. D. Carnes, B. D. Esry, and I. Ben-Itzhak, Phys. Rev. A **84**, 043425 (2011).
[13] H. Liu, Y. Liu, L. Fu, G. Xin, D. Ye, J. Liu, X. T. He, Y. Yang, X. Liu, Y. Deng, C. Wu, and Q. Gong, Phys. Rev. Lett. **109**, 093001 (2012).
[14] U. Eichmann, T. Nubbemeyer, H. Rottke, and W. Sandner, Nature (London) **461**, 1261 (2009).
[15] C. Maher-McWilliams, P. Douglas, and P. F. Barker, Nat. Photon. **6**, 386 (2012).
[16] M. Qiu *et al.*, Science **311**, 1440 (2006).
[17] J. J. Gilijamse, S. Hoekstra, S. Y. T. van de Meerakker, G. C. Groenenboom, and G. Meijer, Science **313**, 1617 (2006).
[18] L. Scharfenberg, S. Y. T. van de Meerakker, and G. Meijer, Phys. Chem. Chem. Phys. **13**, 8448 (2011).
[19] R. V. Krems, Phys. Chem. Chem. Phys. **10**, 4079 (2008).
[20] K. S. Johnson *et al.*, Science **280**, 1583 (1998).
[21] D. Meschede, J. Phys. Conf. Ser. **19**, 118 (2005).
[22] B. P. Anderson and M. A. Kasevich, Science **282**, 1686 (1998).
[23] A. S. Landsman, A. N. Pfeiffer, M. Smolarski, C. Cirelli, and U. Keller, arXiv:1111.6036.
[24] L. B. Fu, G. G. Xin, D. F. Ye, and J. Liu, Phys. Rev. Lett. **108**, 103601 (2012).
[25] L. B. Fu, J. Liu, J. Chen, and S. G. Chen, Phys. Rev. A **63**, 043416 (2001).
[26] L. D. Landau and E. M. Lifshitz, *Quantum Mechanics* (Pergamon Press, New York, 1977).
[27] A. M. Perelomov, V. S. Popov, and V. M. Teren'ev, Zh. Eksp. Teor. Fiz. **52**, 514 (1967) [Sov. Phys. JETP **25**, 336 (1967)]; M. V. Ammosov, N. B. Delone, and V. P. Krainov, Zh. Eksp. Teor. Fiz. **91**, 2008 (1986) [Sov. Phys. JETP **64**, 1191 (1986)]; N. B. Delone and V. P. Krainov, J. Opt. Soc. Am. B **8**, 1207 (1991).
[28] S. P. Goreslavski, G. G. Paulus, S. V. Popruzhenko, and N. I. Shvetsov-Shilovski, Phys. Rev. Lett. **93**, 233002 (2004).
[29] B. Hu, J. Liu, and S. G. Chen, Phys. Lett. A **236**, 533 (1997).
[30] V. P. Krainov, JETP **111**, 171 (2010).